

Comprehensive synthesis and anticoagulant evaluation of a diverse fucoidan library

Received: 10 December 2024

Accepted: 30 April 2025

Published online: 10 May 2025



Si-Cong Chen^{1,5}, Xianjin Qin^{1,2,5}, Nanyu Xiong³, Lisha Lin³, Yanfen Wu¹, Qin Li¹, Dongyue Sun¹, De-Cai Xiong¹, Cassandra E. Callmann⁴, Mingyi Wu³✉ & Xin-Shan Ye¹✉

Fucoidan, a sulfated glycan derived from brown algae, has garnered significant attention for its anticoagulant properties. However, the structural complexity and heterogeneity of naturally extracted fucoidan have hindered a comprehensive understanding of its structure-activity relationship, limiting the development of fucoidan-based anticoagulant drugs. To address this challenge, we synthesize a diverse library of 58 distinct fucoidans with multiple contiguous 1,2-*cis* glycosidic bonds, ranging from disaccharides to dodecasaccharides, using a highly efficient preactivation-based one-pot glycosylation strategy. This library includes compounds with various sulfation patterns (2,3-*O-di*-, 3,4-*O-di*-, and 2,3,4-*O-tri*-sulfation) encompassing nearly all possible fucoidan structures. In vitro anticoagulant assays demonstrate that both molecular size and degree of sulfation play crucial roles in anticoagulant potency. Notably, compounds **29**, **30**, **37**, and **58** significantly prolong human plasma activated partial thromboplastin time (APTT), comparable to the effect of enoxaparin, without affecting prothrombin time (PT) or thrombin time (TT). This selective inhibition of the intrinsic coagulation pathway suggests a reduced risk of bleeding, highlighting the therapeutic potential of these fucoidans as safer anticoagulant agents.

Thrombosis, the formation of blood clots within blood vessels, is the main underlying pathology of cardiovascular diseases, which remain the leading global cause of mortality¹. Anticoagulants are widely used in both medical and surgical settings to manage thrombotic events^{2,3}. Beyond the classical drugs such as heparin and warfarin, a range of heparin derivatives (e.g., enoxaparin and fondaparinux) and direct oral anticoagulants (e.g., dabigatran, rivaroxaban, apixaban, and edoxaban) have been developed. However, all the currently available anticoagulants target coagulation factor Xa (FXa) and/or thrombin (FIIa), which are located in the common pathway, downstream of the coagulation cascade, and are essential to hemostasis function. Despite

their efficacy and widespread use, these anticoagulants are associated with a high risk of bleeding⁴. This prompts researchers to search for safer alternatives. Particularly, emerging evidence underscores the critical role of the intrinsic coagulation pathway in coagulation propagation and thrombosis, while having a limited contribution to hemostasis. Therefore, targeting intrinsic coagulation factors is recognized as a promising strategy for achieving safer and more effective antithrombotic therapies.

Fucoidan, a class of fucose-rich sulfated glycans, are predominantly found in the extracellular matrix of brown algae⁵. These glycans exhibit a wide range of biological activities, including

¹State Key Laboratory of Natural and Biomimetic Drugs, School of Pharmaceutical Sciences, and Chemical Biology Center, Peking University, Beijing, China.

²State Key Laboratory of Natural Medicines, School of Traditional Chinese Pharmacy, China Pharmaceutical University, Nanjing, China. ³State Key Laboratory of Phytochemistry and Natural Medicines, Kunming Institute of Botany, Chinese Academy of Sciences, Kunming, China. ⁴Department of Chemistry, The University of Texas at Austin, Austin, TX, US. ⁵These authors contributed equally: Si-Cong Chen, Xianjin Qin. ✉e-mail: wumingyi@mail.kib.ac.cn;

xinshan@bjmu.edu.cn

anticoagulant⁵, antitumor⁶, anti-inflammatory⁷, and antiviral effects⁸, with anticoagulant activity being one of the most extensively studied^{9–12}. However, the efficacy of fucoidan in anticoagulants varies significantly across different brown algae species, owing to their highly species-specific structures¹³. Currently, most studies on the anticoagulant properties of fucoidan have focused on naturally extracted compounds, which are structurally complex and heterogeneous¹⁴. This heterogeneity has limited the ability to fully understand the structure-activity relationship (SAR) of fucoidan, as access to structurally well-defined fucoidan is challenging. To address this gap and advance the emerging field of fucoidan-based therapeutics, it is crucial to develop a comprehensive collection of structurally well-defined fucoidans with diverse linkages, molecular sizes, and sulfation patterns. Such a library would enable systematic investigation into how structural variations influence biological activities^{15–19}. Over the past two decades, several glycan libraries have been established to explore their functions^{20–25}. Furthermore, strategies have been employed to synthesize fucoidan^{15,17,26,27}, and recent advances in the synthesis of complex polysaccharides have greatly improved our ability to accomplish glycan synthesis^{28–34}. Nevertheless, synthesizing fucoidan with multiple contiguous 1,2-*cis* glycosidic bonds³⁵, coupled with selective *O*-sulfation modifications²³, has continued to pose a considerable challenge.

Herein, we report the development of a fucoidan library utilizing a preactivation-based one-pot glycosylation strategy³⁶. This strategy streamlines synthesis by eliminating the need for intricate leaving group design and laborious intermediate purifications, thus significantly enhancing synthetic efficiency^{36–39}. Through the application of selective *O*-sulfation modifications to the 22 synthesized glycans, ranging from disaccharides to dodecasaccharides, we have constructed a comprehensive library of 58 sulfated fucoidans. This collection encompasses nearly all conceivable fucoidan structures from disaccharides to dodecasaccharides. The comprehensive nature of this library facilitates a systematic investigation of how anticoagulant activity correlates with glycan sizes, linkage types, and sulfation patterns. Notably, unlike enoxaparin, most compounds in the library significantly prolonged activated partial thromboplastin time (APTT) without altering prothrombin time (PT) or thrombin time (TT). These findings indicate that fucoidans selectively inhibit the intrinsic coagulation pathway while sparing the extrinsic and common pathways, potentially reducing the risk of bleeding⁴⁰. As a result, these fucoidans hold the potential as novel anticoagulant agents.

Results

Chemical structures of fucoidans and the general synthetic strategy

The chemical structures of fucoidans vary depending on algal species, cultivation conditions, and extraction methods. Natural fucoidans can be structurally categorized into two primary types (Type A and Type B, Supplementary Fig. 1). Type A, predominantly isolated from *Cladosiphon okamuranus* and *Chorda filum*, features backbones composed of repeating α -(1,3)-linked L-fucopyranosyl residues. In contrast, Type B, primarily derived from *Ascophyllum nodosum* and *Fucus vesiculosus*, consists of backbones with alternating α -(1,3)-linked and α -(1,4)-linked L-fucopyranosyl residues. Although methods such as chemical and enzymatic hydrolysis have been employed to extract fucoidan fragments from natural sources⁴¹, obtaining pure and structurally well-defined fucoidans remains a difficult task. While some fucoidan oligosaccharides have been synthesized in recent decades^{15,17,26,27}, their number and diversity are insufficient to establish a comprehensive structure-activity relationship. To address this issue, we designed a comprehensive fucoidan library comprising 58 compounds, ranging from disaccharides to dodecasaccharides (Fig. 1a). The fucoidans can be classified into two types: Type A (**1–30**), with repeating α -(1,3)-linked L-fucopyranosyl residues, and Type B (**31–58**), with alternating α -(1,3)-linked and α -(1,4)-linked L-fucopyranosyl residues. Importantly, each

type of fucoidans undergoes the late-stage selective *O*-sulfation. Specifically, both Type A and Type B compounds are modified with three sulfation patterns: 2,3-*O*-di-, 3,4-*O*-di-, and 2,3,4-*O*-tri-sulfation. Consequently, the library encompasses most sulfation patterns, spanning from disaccharides to dodecasaccharides.

To facilitate library synthesis (Fig. 1b), we designed several monosaccharide building blocks with a *p*-methylphenylthio (STol) anomeric leaving group, known for its stability and high reactivity in glycosylation^{42–44}. Since all glycosidic linkages constructed in the library are in the 1,2-*cis* configuration, the benzoyl (Bz) group was installed at the 4-*O* position of monosaccharide building blocks to control the anomeric α -stereoselectivity during glycosylation through long-range participation⁴⁵. Super-armed temporary protecting groups, including benzyl (Bn), *tert*-butyldimethylsilyl (TBS), and *p*-methoxybenzyl (PMB), were installed at the 2-*O* and 3-*O* positions to enhance the monosaccharide reactivity and improve the overall glycosylation yield⁴⁶. Furthermore, these orthogonal temporary protecting groups enable the selective removal to expose the desired hydroxyl position for *O*-sulfation.

To efficiently construct the diverse fucoidans, we convergently synthesized two types (Type A and Type B) of glycan backbones (22 protected glycans) from the monosaccharide and oligosaccharide building blocks using the preactivation-based one-pot glycosylation protocol, which maximizes glycan assembly efficiency and reduces the need for tedious intermediate purification steps. The most challenging aspects are the selective deprotection and late-stage sulfation modifications (260 steps for 58 compounds), which involve labor-intensive, multi-step purification of highly polar, charged compounds using silica gel and size-exclusion chromatography. After optimizing sulfation conditions and removing protecting groups, 58 sulfated glycans can be synthesized from the 22 protected glycans by adjusting the order of protecting group removal and sulfation modifications.

Synthesis of monosaccharide and oligosaccharide building blocks

Commercially available L-fucose was selected as the starting material to synthesize all the monosaccharide building blocks (Fig. 2a). Building block **59** was generated through six-step functional group manipulations including successive acetylation, installation of the STol leaving group, deacetylation, selective protection of 3-*O* and 4-*O* with trimethyl orthobenzoate, installation of the Bn group on 2-*O*, and selective partial deprotection of the orthoester. The Bz group at the 4-*O* position of **59** serves both as a temporary protecting group and a stereoselective control element for its long-range participation effect. To obtain the highly reactive glycosyl donor **60**, we installed a TBS group at the 3-*O* position, as the TBS group can improve the reactivity of the glycosyl donor in the glycosylation process, and its protection and deprotection can be achieved in high yields⁴⁶. To prevent palladium catalyst poisoning during benzyl group deprotection and the anomeric hemiacetal hydroxyl group isomerization of the final product, we converted the STol group of **60** into an OMe group, followed by removal of the TBS group to generate the monosaccharide acceptor **61**. For the synthesis of alternating α -(1,3)- and α -(1,4)-linked (Type B) compounds, we employed the PMB group to temporarily protect the hydroxyl group at the 3-*O* position. To achieve this, we first deprotected the 4-*O* Bz group of **59**, and then selectively installed a PMB group at the 3-*O* position using dibutyltin oxide, followed by treatment with PMBCl to obtain the monosaccharide **62**. The same protocol was applied to synthesize the monosaccharide **63** from **61**.

With all the monosaccharides in hand, we began synthesis of the necessary oligosaccharide building blocks to construct the glycan library (Fig. 2b). After optimization of glycosylation conditions (Supplementary Fig. 2), we eventually chose *p*-TolSOTf, generated in situ by *p*-TolSCI and AgOTf, as the promoter to construct the fucosyl α -glycosidic bond. Given that the TBS group in **60** is sensitive to the

Type A series a-1,3 linkage

1-30

2-mer~12-mer

Type B series a-1,3 / a-1,4 alternating linkage

31-58

2-mer~12-mer

<p>1 $a=0, R_1=SO_3^-, R_2=H$</p> <p>2 $a=1, R_1=SO_3^-, R_2=H$</p> <p>3 $a=2, R_1=SO_3^-, R_2=H$</p> <p>4 $a=3, R_1=SO_3^-, R_2=H$</p> <p>5 $a=4, R_1=SO_3^-, R_2=H$</p> <p>6 $a=5, R_1=SO_3^-, R_2=H$</p> <p>7 $a=6, R_1=SO_3^-, R_2=H$</p> <p>8 $a=7, R_1=SO_3^-, R_2=H$</p> <p>9 $a=8, R_1=SO_3^-, R_2=H$</p> <p>10 $a=9, R_1=SO_3^-, R_2=H$</p> <p>11 $a=10, R_1=SO_3^-, R_2=H$</p>	<p>12 $a=0, R_1=H, R_2=SO_3^-$</p> <p>13 $a=1, R_1=H, R_2=SO_3^-$</p> <p>14 $a=2, R_1=H, R_2=SO_3^-$</p> <p>15 $a=3, R_1=H, R_2=SO_3^-$</p> <p>16 $a=4, R_1=H, R_2=SO_3^-$</p> <p>17 $a=5, R_1=H, R_2=SO_3^-$</p> <p>18 $a=6, R_1=H, R_2=SO_3^-$</p> <p>19 $a=7, R_1=H, R_2=SO_3^-$</p> <p>20 $a=8, R_1=H, R_2=SO_3^-$</p> <p>21 $a=9, R_1=H, R_2=SO_3^-$</p> <p>22 $a=10, R_1=H, R_2=SO_3^-$</p>	<p>23 $a=0, R_1=SO_3^-, R_2=SO_3^-$</p> <p>24 $a=1, R_1=SO_3^-, R_2=SO_3^-$</p> <p>25 $a=2, R_1=SO_3^-, R_2=SO_3^-$</p> <p>26 $a=3, R_1=SO_3^-, R_2=SO_3^-$</p> <p>27 $a=4, R_1=SO_3^-, R_2=SO_3^-$</p> <p>28 $a=5, R_1=SO_3^-, R_2=SO_3^-$</p> <p>29 $a=6, R_1=SO_3^-, R_2=SO_3^-$</p> <p>30 $a=8, R_1=SO_3^-, R_2=SO_3^-$</p>	<p>31 $b=1, c=0, R_3=SO_3^-, R_4=H$</p> <p>32 $b=1, c=1, R_3=SO_3^-, R_4=H$</p> <p>33 $b=2, c=0, R_3=SO_3^-, R_4=H$</p> <p>34 $b=2, c=1, R_3=SO_3^-, R_4=H$</p> <p>35 $b=3, c=0, R_3=SO_3^-, R_4=H$</p> <p>36 $b=3, c=1, R_3=SO_3^-, R_4=H$</p> <p>37 $b=4, c=0, R_3=SO_3^-, R_4=H$</p> <p>38 $b=4, c=1, R_3=SO_3^-, R_4=H$</p> <p>39 $b=5, c=0, R_3=SO_3^-, R_4=H$</p> <p>40 $b=5, c=1, R_3=SO_3^-, R_4=H$</p> <p>41 $b=6, c=0, R_3=SO_3^-, R_4=H$</p>	<p>42 $b=1, c=0, R_3=H, R_4=SO_3^-$</p> <p>43 $b=1, c=1, R_3=H, R_4=SO_3^-$</p> <p>44 $b=2, c=0, R_3=H, R_4=SO_3^-$</p> <p>45 $b=2, c=1, R_3=H, R_4=SO_3^-$</p> <p>46 $b=3, c=0, R_3=H, R_4=SO_3^-$</p> <p>47 $b=3, c=1, R_3=H, R_4=SO_3^-$</p> <p>48 $b=4, c=0, R_3=H, R_4=SO_3^-$</p> <p>49 $b=4, c=1, R_3=H, R_4=SO_3^-$</p> <p>50 $b=5, c=0, R_3=H, R_4=SO_3^-$</p> <p>51 $b=5, c=1, R_3=H, R_4=SO_3^-$</p> <p>52 $b=6, c=0, R_3=H, R_4=SO_3^-$</p>	<p>53 $b=1, c=0, R_3=SO_3^-, R_4=SO_3^-$</p> <p>54 $b=1, c=1, R_3=SO_3^-, R_4=SO_3^-$</p> <p>55 $b=2, c=0, R_3=SO_3^-, R_4=SO_3^-$</p> <p>56 $b=2, c=1, R_3=SO_3^-, R_4=SO_3^-$</p> <p>57 $b=3, c=0, R_3=SO_3^-, R_4=SO_3^-$</p> <p>58 $b=3, c=1, R_3=SO_3^-, R_4=SO_3^-$</p>
---	--	---	--	--	---

[illegible]

trifluoromethanesulfonic acid (TfOH) byproduct that is produced during the glycosylation, the sterically-hindered acid scavenger 2,4,6-*tert*-butylpyrimidine (TTBP) was added into the reaction mixture. Glycosyl donor **60** was first preactivated with *p*-TolSCl/AgOTf in the presence of TTBP, and then reacted with acceptor **59**, resulting in disaccharide **64** in 91% isolated yield. The long-range participation of the 4-*O* Bz group led to excellent α -selectivity, which was confirmed by $^1\text{H-NMR}$ ($J_{\text{H1-H2}} = 3.0$ Hz) and HMBC ($J_{\text{H1-C1}} = 168$ Hz) (Supplementary Fig. 3). Removal of the TBS group from the 3-*O* position of disaccharide **64** using HF-pyridine produced disaccharide acceptor **65** in excellent yield. The same protocol was used to synthesize disaccharide **66** by the coupling of glycosyl donor **60** with acceptor **61** in 93% yield, followed by subsequent deprotection of TBS, which afforded the disaccharide acceptor **67** in high yield. For Type B fucoidan synthesis, two α -(1,4)-linked disaccharide building blocks (**69** and **71**) were prepared by a similar approach (Fig. 2c). We found that the formation of the α -(1,4) linkage was slightly more challenging than the α -(1,3) linkage; therefore, we increased the temperature of the glycosylation from -78°C to -72°C . Due to the presence of the PMB group and the increased glycosylation temperature, the equivalents of TTBP used were increased from 1.2 to 1.3 to mitigate PMB group instability during glycosylation. Eventually, α -(1,4) disaccharides **68** and **70** were successfully synthesized by coupling of **60** with **62** and **63**, respectively, again utilizing the *p*-TolSCl/AgOTf promoter system. Lastly, the two disaccharide acceptors **69** and **71** were generated by deprotection of the TBS groups at 3-*O* position of **68** and **70** using HF-pyridine. The anomeric α -configuration of the newly formed 1,4-linkage was confirmed by its $^1\text{H-NMR}$ ($J_{\text{H1-H2}} = 3.3$ Hz) and HMBC ($J_{\text{H1-C1}} = 167$ Hz) (Supplementary Fig. 4).

3

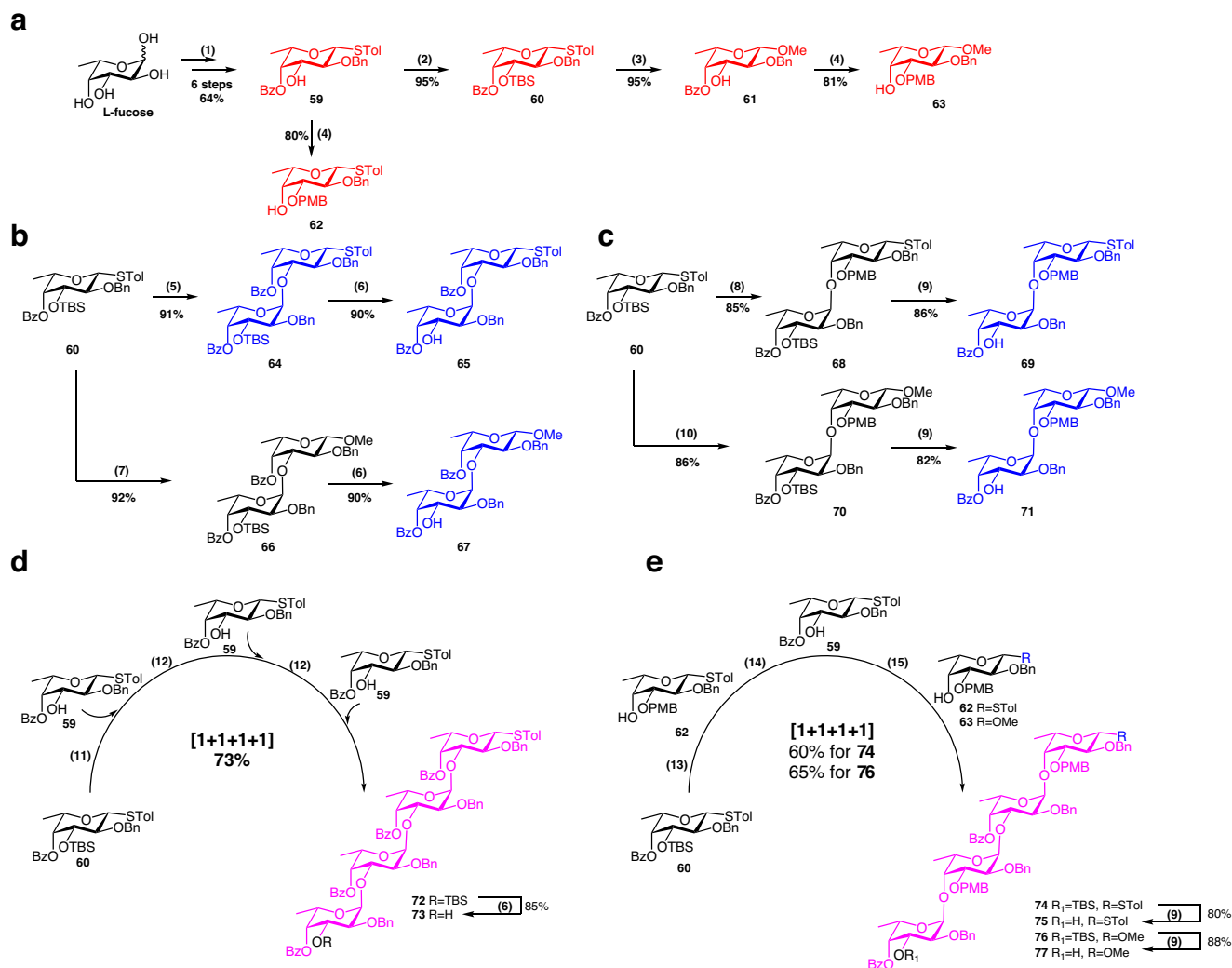


Fig. 2 | Synthesis of the monosaccharide and oligosaccharide building blocks.

a Synthesis of monosaccharides **59–63**. **b** Synthesis of disaccharides **64**, **65**, and **67**. **c** Synthesis of disaccharide acceptors **69** and **71**. **d** Synthesis of tetrasaccharides **72** and **73**. **e** Synthesis of tetrasaccharides **74**, **75**, and **77**. Reagents and conditions: (1) (a) Ac_2O , HClO_4 , 0°C , 1 h; (b) $p\text{-TolSH}$, $\text{BF}_3\cdot\text{OEt}_2$, DCM, 0°C to rt; (c) NaOCH_3 , CH_3OH , rt, 1 h; (d) $\text{PhC}(\text{OCH}_3)_3$, CSA, MeCN, rt, 3 h; (e) BnBr , NaH, DMF, 0°C , 3 h; (f) 1 N HCl, rt, 1 h; (2) TBSCl, imidazole, DMF, 70°C , 4 h; (3) (a) CH_3OH , 4 Å MS, $p\text{-TolSCI}$, AgOTf, TTBP, DCM, -78°C to rt, 1 h; (b) HF-pyridine, THF, 50°C , 4 h; (4) (a) NaOCH_3 , CH_3OH , 50°C , 1 h; (b) Bu_2SnO , toluene, 120°C , 6 h; (c) PMBCl, CsF, DMF, 70°C , 4 h; (5) TTBP, 4 Å MS, DCM, $p\text{-TolSCI}$, AgOTf, then **59**, -78°C to rt, 1.5 h; (6) HF-pyridine, THF, 50°C , 4 h; (7) TTBP, 4 Å MS, DCM, $p\text{-TolSCI}$, AgOTf, then **61**, -78°C to rt, 1.5 h; (8) TTBP, 4 Å MS, DCM, $p\text{-TolSCI}$, AgOTf, then **62**, -72°C to rt, 1.5 h; (9) HF-pyridine, THF, 45°C , 6 h; (10) TTBP, 4 Å MS, DCM, $p\text{-TolSCI}$, AgOTf, then **63**, -72°C to rt, 1.5 h; (11) TTBP, 4 Å MS, DCM, $p\text{-TolSCI}$, AgOTf, then **59**, -78°C to rt, 1.5 h; (12) $p\text{-TolSCI}$, AgOTf, then **59**, -78°C to rt, 1.5 h; (13) TTBP, 4 Å MS, DCM, $p\text{-TolSCI}$, AgOTf, then **62**, -72°C to rt, 1.5 h; (14) $p\text{-TolSCI}$, AgOTf, then **59**, -72°C to rt, 1.5 h; (15) $p\text{-TolSCI}$, AgOTf, then **62** or **63**, -72°C to rt, 1.5 h. Tol, $p\text{-methylphenyl}$; Bz, benzoyl; Bn, benzyl; TBS, *tert*-butyldimethylsilyl; PMB, *p*-methoxybenzyl; TTBP, 2,4,6-*tri-tert*-butylpyrimidine; MS, molecular sieves.

(6) HF-pyridine, THF, 50°C , 4 h; (7) TTBP, 4 Å MS, DCM, $p\text{-TolSCI}$, AgOTf, then **61**, -78°C to rt, 1.5 h; (8) TTBP, 4 Å MS, DCM, $p\text{-TolSCI}$, AgOTf, then **62**, -72°C to rt, 1.5 h; (9) HF-pyridine, THF, 45°C , 6 h; (10) TTBP, 4 Å MS, DCM, $p\text{-TolSCI}$, AgOTf, then **63**, -72°C to rt, 1.5 h; (11) TTBP, 4 Å MS, DCM, $p\text{-TolSCI}$, AgOTf, then **59**, -78°C to rt, 1.5 h; (12) $p\text{-TolSCI}$, AgOTf, then **59**, -78°C to rt, 1.5 h; (13) TTBP, 4 Å MS, DCM, $p\text{-TolSCI}$, AgOTf, then **62**, -72°C to rt, 1.5 h; (14) $p\text{-TolSCI}$, AgOTf, then **59**, -72°C to rt, 1.5 h; (15) $p\text{-TolSCI}$, AgOTf, then **62** or **63**, -72°C to rt, 1.5 h. Tol, $p\text{-methylphenyl}$; Bz, benzoyl; Bn, benzyl; TBS, *tert*-butyldimethylsilyl; PMB, *p*-methoxybenzyl; TTBP, 2,4,6-*tri-tert*-butylpyrimidine; MS, molecular sieves.

3-*O* position of tetrasaccharides **74** and **76** produced tetrasaccharide glycosyl acceptors **75** and **77**, respectively.

One-pot assembly of protected Type A and Type B glycans

Equipped with a comprehensive set of monosaccharides and oligosaccharides, we then aimed to construct a diverse fucoidan library with high efficiency using the preactivation-based one-pot glycosylation strategy (Fig. 3). In the synthesis of Type A compounds (Fig. 3a), we utilized monosaccharides **60**, **59**, and **61**. Trisaccharide **78** was synthesized in 81% overall yield via a one-pot three-component [1 + 1 + 1] glycosylation, promoted by $p\text{-TolSCI}$ /AgOTf. Subsequent removal of the TBS group at 3-*O* position using HF-pyridine yielded trisaccharide acceptor **79** in 91% yield. Similarly, tetrasaccharide **80** was obtained in 72% yield through a one-pot four-component [1 + 1 + 1 + 1] glycosylation. The TBS group deprotection at 3-*O* position provided tetrasaccharide **81** in 90% yield. For pentasaccharide **82**, a one-pot three-

component [2 + 1 + 2] glycosylation was performed using disaccharide **64**, monosaccharide **59**, and disaccharide acceptor **67**, achieving an 81% overall yield. Following TBS removal, pentasaccharide acceptor **83** was obtained in 88% yield. Hexasaccharide **84** was assembled via a one-pot three-component [2 + 2 + 2] glycosylation utilizing disaccharide donor **64**, acceptors **65** and **67**, resulting in an 80% overall yield. Deprotection with HF-pyridine produced hexasaccharide **85** in 95% yield. Heptasaccharide **86** was synthesized through a one-pot three-component [4 + 1 + 2] glycosylation, starting from tetrasaccharide **72**, monosaccharide **59**, and disaccharide **67**, in a 76% overall yield. The subsequent TBS deprotection yielded heptasaccharide **87** in 87% yield. Octasaccharide **88** was prepared via a one-pot four-component [2 + 2 + 2 + 2] glycosylation with disaccharides **64**, **65** (two additions) and **67**, achieving a 65% yield. TBS deprotection afforded octasaccharide **89** in 92% yield. Nonsaccharide **90** was synthesized in 62% yield using a one-pot four-component [4 + 2 + 2 + 1] glycosylation,

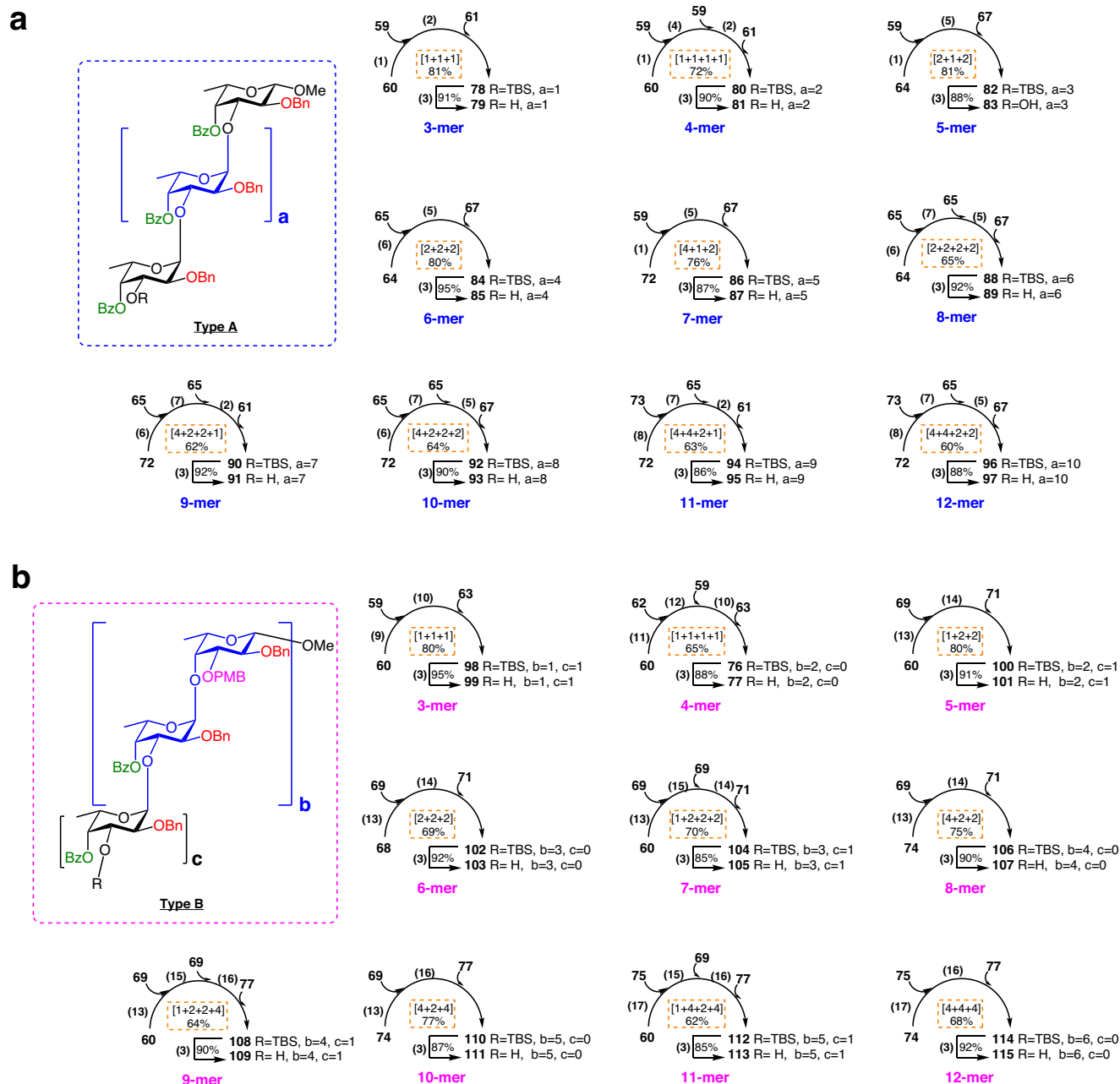


Fig. 3 | Assembly of fully protected glycans by preactivation-based one-pot glycosylation strategy. a Synthesis of Type A glycans. **b** Synthesis of Type B glycans. (1) TTBP, 4 Å MS, DCM, *p*-TolSCI, AgOTf, then **59**, –78 °C to rt, 1.5 h; (2) *p*-TolSCI, AgOTf, then **61**, –78 °C to rt, 1.5 h; (3) HF-pyridine, THF, 50 °C, 4 h; (4) *p*-TolSCI, AgOTf, then **59**, –78 °C to rt, 1.5 h; (5) *p*-TolSCI, AgOTf, then **67**, –78 °C to rt, 1.5 h; (6) TTBP, 4 Å MS, DCM, *p*-TolSCI, AgOTf, then **65**, –78 °C to rt, 1.5 h; (7) *p*-TolSCI, AgOTf, then **65**, –78 °C to rt, 1.5 h; (8) TTBP, 4 Å MS, DCM, *p*-TolSCI, AgOTf, then **73**, –78 °C to rt, 1.5 h; (9) TTBP, 4 Å MS, DCM, *p*-TolSCI, AgOTf, then **59**, –72 °C

to rt, 1.5 h; (10) *p*-TolSCI, AgOTf, **63**, –72 °C to rt, 1.5 h; (11) TTBP, 4 Å MS, DCM, *p*-TolSCI, AgOTf, then **62**, –72 °C to rt, 1.5 h; (12) *p*-TolSCI, AgOTf, then **59**, –72 °C to rt, 1.5 h; (13) TTBP, 4 Å MS, DCM, *p*-TolSCI, AgOTf, then **69**, –72 °C to rt, 1.5 h; (14) *p*-TolSCI, AgOTf, then **71**, –72 °C to rt, 1.5 h; (15) *p*-TolSCI, AgOTf, then **69**, –72 °C to rt, 1.5 h; (16) *p*-TolSCI, AgOTf, then **77**, –72 °C to rt, 1.5 h; (17) TTBP, 4 Å MS, DCM, *p*-TolSCI, AgOTf, then **75**, –72 °C to rt, 1.5 h. Tol, *p*-methylphenyl; Bz, benzoyl; Bn, benzyl; TBS, *tert*-butyldimethylsilyl; PMB, *p*-methoxybenzyl; TTBP, 2,4,6-*tri*-*tert*-butylpyrimidine; MS, molecular sieves.

starting from tetrasaccharide **72**, disaccharide **65** (two additions), and monosaccharide **61**. Removal of the TBS group produced nonasaccharide **91** in 92% yield. Decasaccharide **92** was constructed via a one-pot four-component [4 + 2 + 2 + 2] glycosylation, utilizing tetrasaccharide **72**, disaccharide **65** (two additions), and disaccharide **67**, resulting in a 64% overall yield. The TBS deprotection gave decasaccharide **93** in 90% yield. Undecasaccharide **94** was synthesized through a one-pot four-component [4 + 4 + 2 + 1] glycosylation in 63% yield from tetrasaccharide **72**, tetrasaccharide **73**, disaccharide **65**, and

monosaccharide **61**. The TBS group removal produced undecasaccharide **95** in 86% yield. Finally, dodecasaccharide **96** was synthesized using a one-pot four-component [4 + 4 + 2 + 2] glycosylation, starting from tetrasaccharide donor **72**, tetrasaccharide acceptor **73**, disaccharide acceptors **65** then **67**, achieving a 60% overall yield. Deprotection of the TBS group at the 3-O position afforded dodecasaccharide **97** in 88% yield.

For the synthesis of Type B compounds (Fig. 3b), we again employed the preactivation-based one-pot glycosylation strategy,

which we have already successfully utilized in the synthesis of Type A compounds. Our preliminary studies revealed that the efficiency of the α -(1,4) glycosylation reaction was significantly diminished compared to α -(1,3)-glycosylation, especially when the molecular size of the glycosyl donors and acceptors was increased. To address this issue, we designed our synthetic route such that the α -(1,4) linkages would be formed with higher efficiency at the disaccharide level, and then we would use these intermediates to further construct the subsequent α -(1,3) linkages. Throughout the synthesis of the 10 fully protected glycans, ranging from trisaccharide to dodecasaccharide, *p*-TolSCI/AgOTf was consistently identified as the optimal promoter for all glycosylation reactions. Specifically, trisaccharide **98** was synthesized via a one-pot three-component [1 + 1 + 1] glycosylation, achieving an 80% overall yield from monosaccharide donor **60** and monosaccharide acceptors **59** then **63**. Tetrasaccharide **76** was produced through a one-pot four-component [1 + 1 + 1 + 1] glycosylation from monosaccharide donor **60** and monosaccharide acceptors **62**, **59**, then **63**. Pentasaccharide **100** was assembled in 80% yield by a one-pot three-component [1 + 2 + 2] approach from monosaccharide **60** and disaccharides **69** then **71**. Hexasaccharide **102** was synthesized by a one-pot three-component [2 + 2 + 2] glycosylation, with an overall yield of 69% from disaccharides **68**, **69**, and **71**. Heptasaccharide **104** was assembled using a one-pot four-component [1 + 2 + 2 + 2] strategy, achieving a 70% overall yield from monosaccharide donor **60**, and disaccharide acceptors **69** then **71**. Octasaccharide **106** was synthesized via a one-pot three-component [4 + 2 + 2] approach in 75% overall yield from tetrasaccharide donor **74**, and disaccharide acceptors **69** then **71**. Nonasaccharide **108** was constructed by a one-pot four-component

[1 + 2 + 2 + 4] glycosylation, in 64% overall yield from monosaccharide donor **60**, disaccharide acceptor **69**, and lastly tetrasaccharide acceptor **77**. Decasaccharide **110** was assembled through a one-pot three-component [4 + 2 + 4] glycosylation, achieving a 77% overall yield from tetrasaccharide donor **74**, disaccharide acceptor **69**, then tetrasaccharide acceptor **77**. Undecasaccharide **112** was synthesized using a one-pot four-component [1 + 4 + 2 + 4] strategy in 62% overall yield from monosaccharide donor **60**, tetrasaccharide acceptor **75**, disaccharide acceptor **69**, and tetrasaccharide acceptor **77**. Finally, dodecasaccharide **114** was assembled by a one-pot three-component [4 + 4 + 4] glycosylation, with a 68% overall yield from tetrasaccharide donor **74**, and tetrasaccharide acceptors **75** then **77**. Lastly, the TBS group at the 3-O position of all assembled glycans, from trisaccharide **98** to dodecasaccharide **114**, was effectively removed using HF-pyridine to afford the corresponding oligosaccharides **99** to **115**, achieving yields ranging from 85% to 95%.

Divergent synthesis of the fucoidan library

To investigate the impact of sulfation patterns on the anticoagulant activity of fucoidan, we modified both Type A and Type B glycans with three distinct sulfation patterns: 2,3-*O*-di-, 3,4-*O*-di-, and 2,3,4-*O*-tri-sulfation. Glycans **67** and **79–97**, synthesized by a preactivation-based one-pot glycosylation strategy, served as the precursors for constructing the differentially sulfated Type A fucoidans. To prepare the 2,3-*O*-di-sulfated compounds (Fig. 4), referring to the reported orthogonal deprotection strategy^{15,17}, the protected glycans first underwent hydrogenolysis using palladium hydroxide under a 0.4 MPa H₂ atmosphere to remove all Bn groups at the 2-O position, yielding

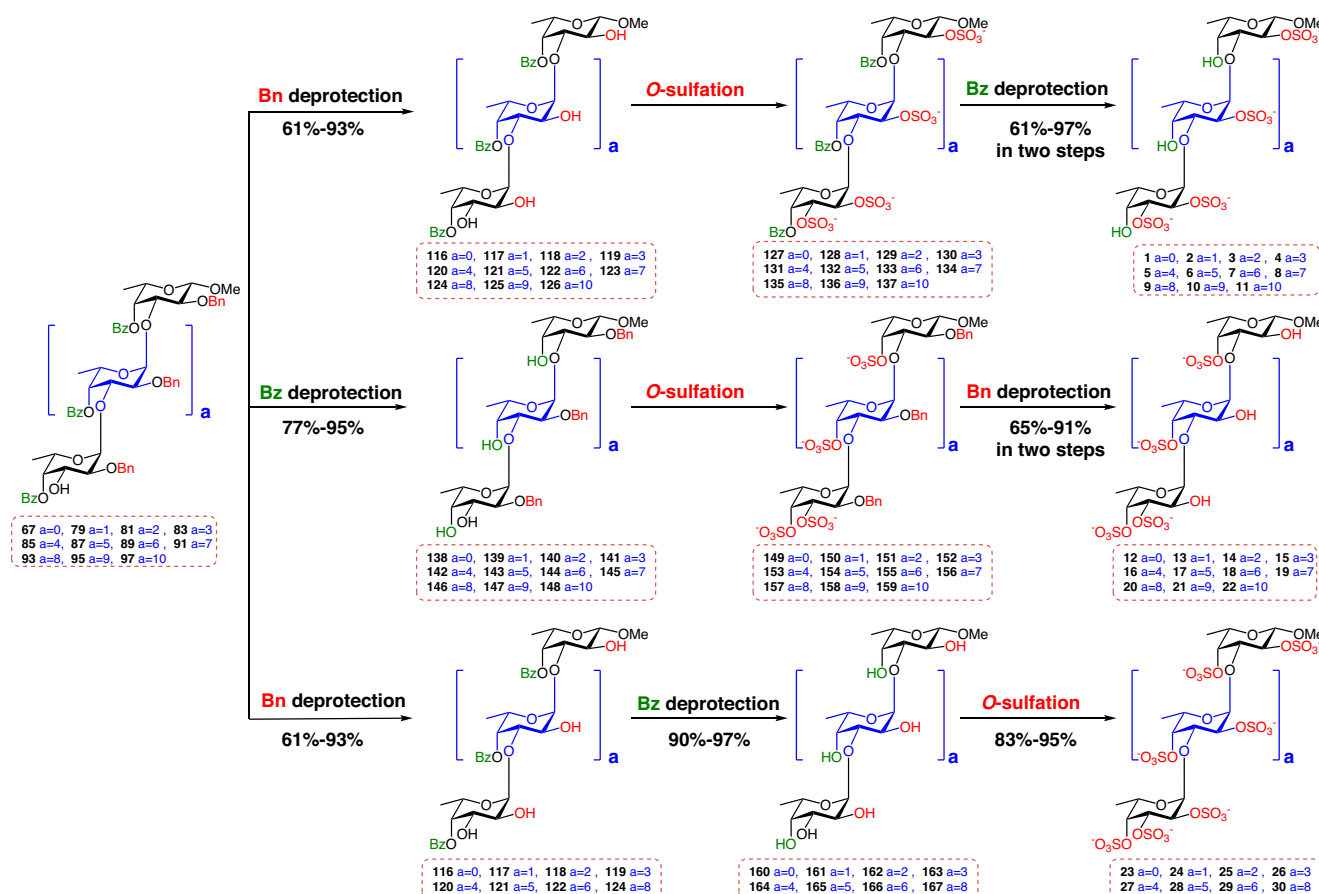


Fig. 4 | Protecting group deprotection and late-stage selective O-sulfation for Type A compounds. Conditions for deprotection of Bz group: KOH, THF/MeOH = 3:1; or 3 M NaOH or NaOCH₃, CH₃OH; Conditions for deprotection of

Bn group: 0.4 MPa H₂, Pd(OH)₂/C, ethyl acetate/MeOH = 1:1; Conditions for O-sulfation: SO₃-NMe₃, DMF; or SO₃-pyridine, DMF. Bz, benzoyl; Bn, benzyl.

intermediates **116–126** in considerable yields. Initially, a mixed solvent of ethyl acetate and methanol in a 1:1 ratio was employed for hydrolysis across glycans ranging from the trisaccharide to the heptasaccharide. However, this solvent proved to be inadequate for solubilizing the octasaccharide and larger glycans. After optimization of the reaction conditions, we found that a slightly more polar mixed solvent of ethyl acetate and methanol in a 1:1.5 ratio facilitated more efficient reactions for larger glycans. After acquiring the intermediates **116–126**, we then focused on the *O*-sulfation modification. Given the high polarity of the products and the sensitivity of the sulfation reaction to trace amounts of moisture, real-time monitoring via TLC was not feasible. Instead, we employed NMR and HRMS to trace the purified sulfation products. Initially, we selected sulfur trioxide triethylamine complex ($\text{SO}_3\text{-NEt}_3$) as the sulfation reagent to achieve 2,3-*O*-disulfation. However, certain hydroxyl groups proved difficult to sulfate, leading to incomplete sulfation in many cases. After optimizing the sulfation conditions, we utilized 15 equivalents per hydroxyl group of the less sterically hindered sulfur trioxide trimethylamine complex ($\text{SO}_3\text{-NMe}_3$) as the sulfation reagent to achieve complete sulfation. Following purification by size exclusion chromatography, the sulfated intermediates **127–137** were treated with sodium hydroxide solution to deprotect the Bz groups. Simultaneously, the products in the form of ammonium salts were converted to the products in the form of sodium salts, resulting in 2,3-*O*-di-sulfated fucoidans **1–11** in quantitative yields.

To achieve the synthesis of 3,4-*O*-di-sulfated fucoidans, we initially treated the protected Type A glycans (**67** and **79–97**) with sodium methoxide in methanol to remove the Bz groups. However, the poor solubility of the relatively non-polar protected glycans in methanol impeded the complete removal of the Bz groups, even when employing a mixed solvent of tetrahydrofuran and methanol. After

optimizing the conditions, we successfully dissolved the glycans in a mixed solvent of tetrahydrofuran and methanol (3:1) and deprotected the Bz groups using potassium hydroxide. This approach ensured quantitative removal of Bz groups, resulting in intermediates **138–148**. Following the sulfation protocol described above for 2,3-*O*-disulfation, sulfate groups were installed at the 3,4-*O* positions of **138–148** to afford sulfated intermediates **149–159**. Lastly, hydrogenolysis with palladium hydroxide under a 0.4 MPa H_2 atmosphere was accomplished to remove the Bn groups, which was followed by treatment with 3 M NaOH, yielding the 3,4-*O*-di-sulfated fucoidans **12–22**.

To synthesize 2,3,4-*O*-tri-sulfated fucoidans, intermediates **116–124** were utilized as starting materials. The Bz groups on these intermediates were first deprotected via treatment with sodium methoxide in methanol, yielding fully unprotected glycans **160–167** in quantitative yields. The primary challenge in this series of compounds was the subsequent sulfation of all hydroxyl groups present due to both the increased steric hindrance and the increased electrostatic repulsion accumulating throughout the sulfation process, compared to single-site sulfation. In addition, when exposed to prolonged reaction time, we observed partial decomposition of these fucoidans. Ultimately, SO_3 -pyridine was chosen as the sulfation reagent, with DMF as the solvent. The reaction was conducted at room temperature for 14 h, successfully yielding fully sulfated fucoidans. However, achieving complete sulfation remained challenging for glycans larger than decasaccharide, despite increased reaction temperatures and extended reaction times. After purification of the fully sulfated fucoidans, the products were treated with sodium hydroxide to produce the sodium salts **23–30**.

The protected Type B glycans were initially subjected to TfOH in dichloromethane for the rapid deprotection of PMB groups, providing compounds **168–178** in 74–91% yields (Fig. 5). Subsequently, removal

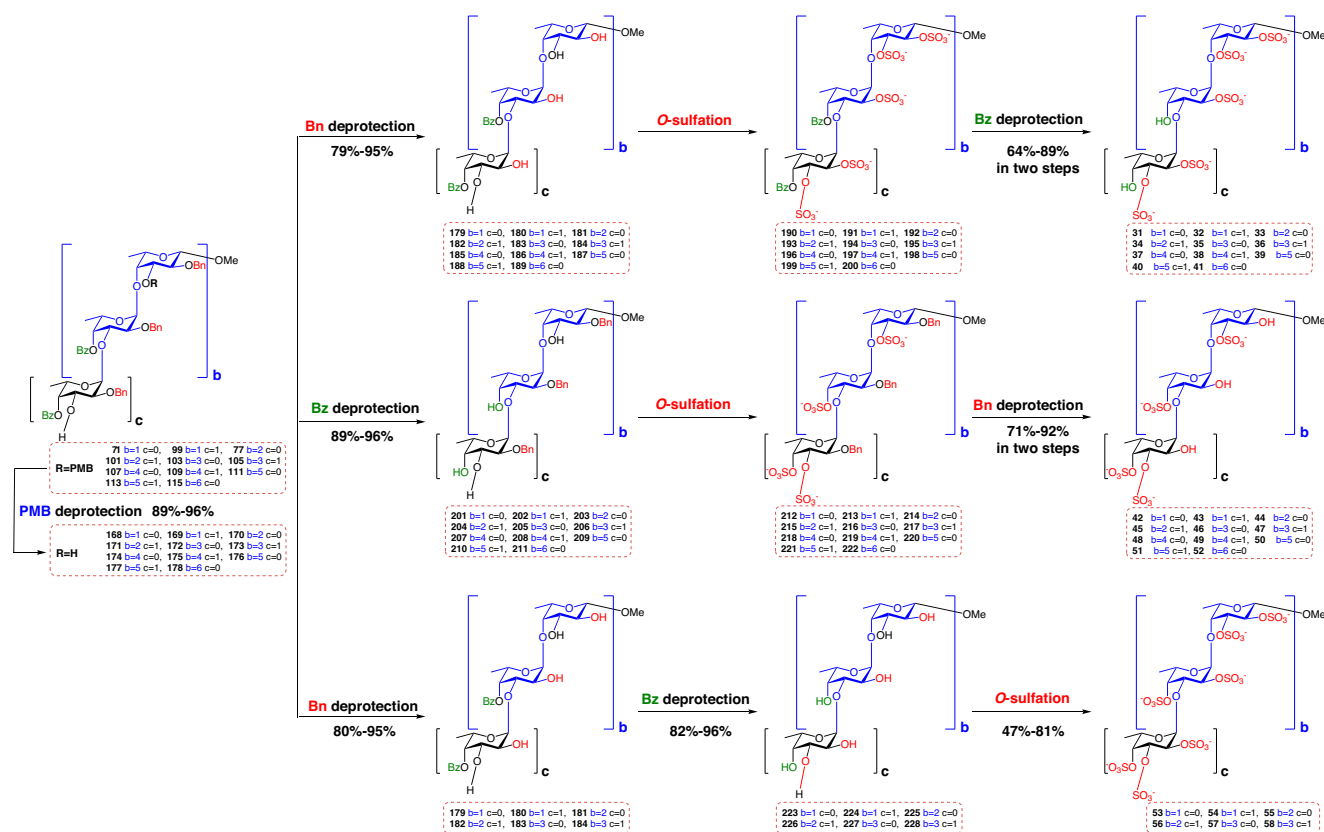


Fig. 5 | Protecting group deprotection and late-stage selective *O*-sulfation for Type B compounds. Conditions for deprotection of PMB group: TfOH/DCM = 1:10; conditions for deprotection of Bz group: KOH, THF/MeOH = 3:1; or 3 M NaOH; or NaOCH₃, MeOH; conditions for deprotection of Bn group: 0.4 MPa H_2 , Pd(OH)₂/C,

ethyl acetate/MeOH=1:1 or ethyl acetate/MeOH = 1:1.5 or $\text{H}_2\text{O}/\text{MeOH} = 1:1$; conditions for *O*-sulfation: $\text{SO}_3\text{-NMe}_3$, DMF; or SO_3 -pyridine, DMF; Bz, benzoyl; Bn, benzyl; PMB, *p*-methoxybenzyl.

of the Bn groups by hydrogenolysis under palladium hydroxide in a 0.4 MPa H₂ atmosphere afforded intermediates **179–189**. During the hydrogenolysis process, a mixed solvent (ethyl acetate and methanol in a 1:1 ratio) ensured the solubility of substrates up to non-asaccharide. For larger glycans, the solvent ratio was slightly altered (ethyl acetate and methanol 1:1.5). The 2,3-*O*-di-sulfation modification commenced with the treatment of intermediates **179–189** using SO₃-pyridine. After purification via size exclusion chromatography, intermediates **190–200** were obtained, which were treated with sodium hydroxide solution to remove the Bz groups and convert the pyridinium sulfate salts into the sodium salts, resulting in the formation of 2,3-*O*-di-sulfated products **31–41**. To construct 3,4-*O*-di-sulfated glycans, protected glycans **168–178** were used as starting materials. Treatment with potassium hydroxide facilitated the removal of the Bz groups present, affording intermediates **201–211** in quantitative yields, which were followed by sulfation with SO₃-pyridine, affording compounds **212–222**. After acquiring sulfated intermediates, hydrogenolysis of all the Bn groups at 2-*O* position under palladium hydroxide generated 3,4-*O*-di-sulfated pyridinium salts, which, after treatment with sodium hydroxide solution, yielded 3,4-*O*-di-sulfated sodium salts **42–52**. The most challenging aspect of constructing the Type B fucoidan compounds was the synthesis of 2,3,4-*O*-tri-sulfated products. After obtaining fully unprotected glycans **223–228** in quantitative yield from **179–184** via treatment with NaOMe/MeOH, we meticulously optimized parameters critical to achieving complete sulfation, including the choice of sulfation reagent, temperature, reaction duration, solvent, and concentration. Ultimately, we found that SO₃-pyridine was the most effective reagent for sulfation of glycans up to heptasaccharide, yielding 2,3,4-*O*-tri-sulfated products **53–58**. For larger glycans, achieving complete sulfation proved difficult due to frequent incomplete sulfation and

glycan decomposition, thereby hindering the synthesis of the larger desired 2,3,4-*O*-tri-sulfated products.

Evaluation of anticoagulant activity

Having synthesized a structurally homogeneous and well-defined library of fucoidan sulfates, we aimed to evaluate their anticoagulant activity and investigate the structure-activity relationships. The 58 precisely synthesized fucoidan sulfate compounds were evaluated for their effects on activated partial thromboplastin time (APTT), prothrombin time (PT), and thrombin time (TT) using human plasma, reflecting their influence on the intrinsic, extrinsic, and common coagulation pathways, respectively (Fig. 6a and Supplementary Tables S1–S3). The results revealed that at a concentration of 128 µg/mL, compounds **25, 26, 27, 28, 29, 30, 35, 36, 37, 38, 39, 40, 41, 56, 57**, and **58** significantly prolonged APTT to at least twice that of the control group. Notably, compounds **28, 29, 30, 37**, and **58** demonstrated the most potent efficacy, prolonging APTT to over 12 folds compared to the control group, indicating potent inhibition of the intrinsic coagulation pathway. In contrast, at the same concentration, none of the compounds **1–58** exhibited significant effects on prolonging either PT or TT, suggesting that these fucoidans exert negligible inhibitory activity towards the extrinsic coagulation pathway and common coagulation pathway. Whereas, the positive control, enoxaparin at 4 µg/mL extended TT to 3.5 folds compared to the control group. Taken together, these findings underscore that certain chemically synthesized fucoidans have a distinct anticoagulant mechanism, they selectively inhibit the intrinsic coagulation pathway, with minimal effects on the extrinsic and common pathways.

To further investigate the inhibitory effects of the fucoidan sulfates on intrinsic coagulation, the concentrations of compounds

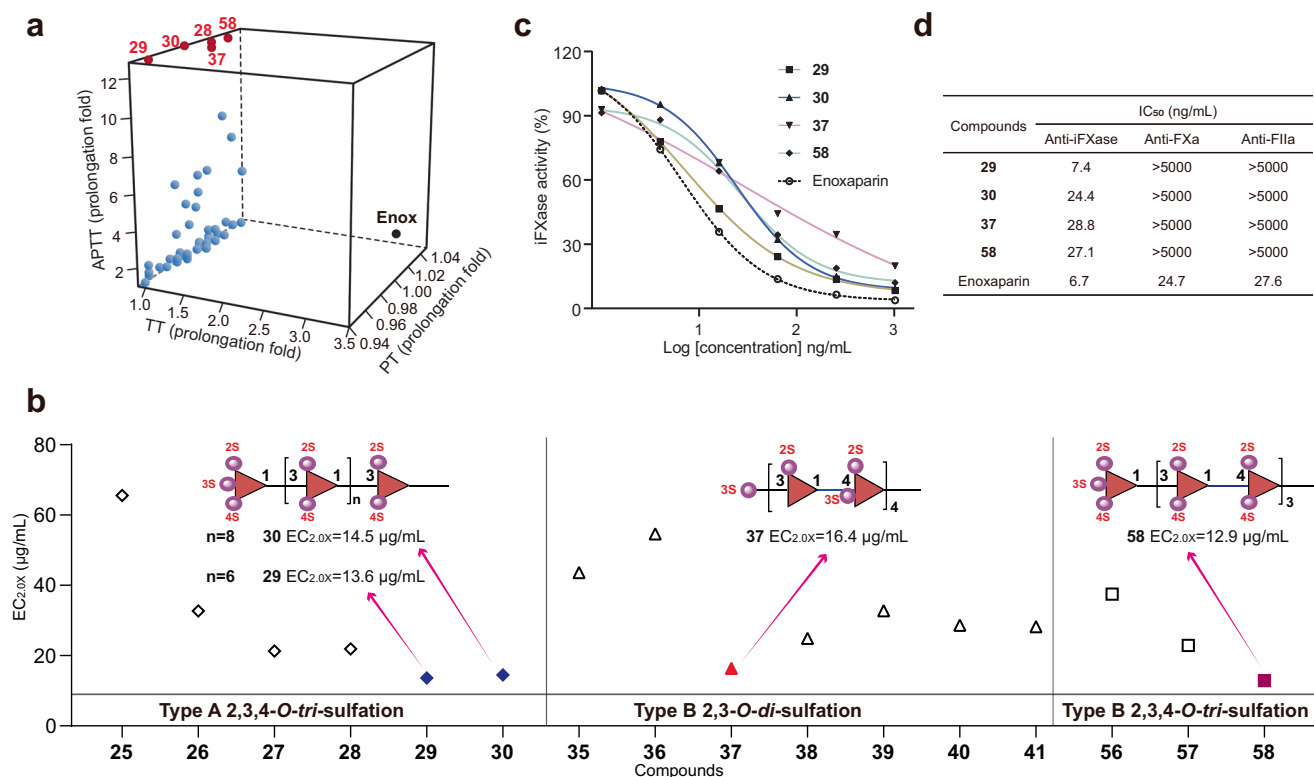


Fig. 6 | Anticoagulant evaluation of fucoidan library. **a** Effects of the fucoidans on the prolongation of APTT, TT, and PT. Fucoidans were all at 128 µg/mL, Enox was at 4, 16, and 100 µg/mL for TT, APTT, and PT, respectively. Experiments were conducted in triplicate, and mean values were presented. **b** EC_{2.0x} values of active fucoidans, assessing their inhibition of the intrinsic coagulation pathway by APTT.

c Effects of the most potent compounds (**29, 30, 37**, and **58**) on intrinsic coagulation factor Xase (iFXase) activity. Experiments were conducted in duplicate, and data were presented as mean. **d** IC₅₀ values of **29, 30, 37**, and **58** against iFXase and their effects on FXa and FIIa in the presence of antithrombin. APTT, activated partial thromboplastin time; PT, prothrombin time; TT, thrombin time.

required for doubling APTT ($EC_{2.0\times}$) were determined (Fig. 6b and Supplementary Fig. 6). Compounds **29**, **30**, **37**, and **58** exhibited potent activity with $EC_{2.0\times}$ values of 13.6 $\mu\text{g/mL}$, 14.5 $\mu\text{g/mL}$, 16.4 $\mu\text{g/mL}$, and 12.9 $\mu\text{g/mL}$, respectively, which are comparable to that of enoxaparin ($EC_{2.0\times}$ value of 7.0 $\mu\text{g/mL}$). By analyzing the structures and APTT-prolonging anticoagulant activities of the 58 fucoidan sulfate compounds, we found that for Type A compounds, the 2,3,4-*O*-tri-sulfation modification significantly enhanced anticoagulant activity. For Type B compounds, both 2,3-*O*-di-sulfation and 2,3,4-*O*-tri-sulfation modifications exhibited superior anticoagulant effects. These findings suggest that while the degree of sulfation significantly contributes to the anticoagulant efficacy of fucoidan sulfates, the connectivity of the glycosidic bonds also plays a role. In addition, we observed that, for 2,3,4-*O*-tri-sulfation modification, the anticoagulant activity was enhanced with the increase of molecular size.

We conducted a detailed investigation into the anticoagulant mechanism of the most promising compounds **29**, **30**, **37**, and **58**. Specifically, we assessed their effects on intrinsic coagulation factor Xase (iFXase) activity, a critical rate-limiting enzyme in the intrinsic pathway⁵². In addition, we evaluated their impact on the activities of factor Xa (FXa) and thrombin (factor IIa, FIIa) in the presence of antithrombin (AT), given that heparin-like anticoagulants exert their effects by AT-mediated inhibition of FXa and FIIa. Compounds **29**, **30**, **37**, and **58** demonstrated potent, concentration-dependent inhibition of iFXase within the range of 4–4096 ng/mL. Notably, compound **29** exhibited an IC_{50} value of 7.4 ng/mL, closely aligning with that of enoxaparin (IC_{50} = 6.7 ng/mL). Moreover, compounds **30**, **37**, and **58** demonstrated considerable anti-iFXase activity, with IC_{50} values of 24.4 ng/mL, 28.8 ng/mL, and 27.1 ng/mL, respectively (Fig. 6c). In the presence of AT, these compounds did not inhibit FXa or FIIa activities, with IC_{50} values all exceeding 5000 ng/mL. In contrast, the positive control, enoxaparin, exhibited IC_{50} values of 24.7 ng/mL for FXa and 27.6 ng/mL for FIIa (Fig. 6d and Supplementary Figs. 7, 8). These findings suggest that compounds **29**, **30**, **37**, and **58** inhibited the intrinsic coagulation pathway by selectively targeting iFXase in an AT-independent manner. This indicates that their anticoagulant mechanism is distinct from those of heparin-like molecules. In addition, taking compound **37** as an example, its superior anticoagulant activity could be explained by molecular docking simulations that simulated the interactions between FIXa (the key enzyme of iFXase complex) and the compound (Supplementary Figs. 9–12). To evaluate the safety profiles of the four compounds, we also tested the cytotoxicity of these compounds on two cell lines, RAW246.7 and NIH 3T3. The results showed that the compounds exhibited negligible cytotoxicity even at a high concentration of 128 $\mu\text{g/mL}$ (Supplementary Figs. 13, 14). This indicates that these compounds are likely to be safe for their intended applications.

The fucoidan sulfates we have developed selectively inhibit the intrinsic coagulation pathway without interfering with the extrinsic and common pathways. By specifically targeting iFXase, the rate-limiting enzyme complex in the intrinsic coagulation pathway, our compounds enable safe and effective antithrombosis. This is particularly crucial for patients requiring long-term anticoagulant therapy, such as those with chronic conditions like venous thromboembolism. This targeted approach is particularly beneficial for patients who may have contraindications or intolerances to extrinsic pathway inhibitors like warfarin. Thus, selective inhibition of the intrinsic pathway provides a valuable alternative for patients who need tailored anticoagulant therapy.

Discussion

By utilizing a preactivation-based one-pot glycosylation strategy, we have efficiently and expeditiously assembled a comprehensive library of sulfated fucoidan compounds. This library comprises 58 distinct molecules, ranging from disaccharides to dodecasaccharides,

incorporating three diverse sulfation patterns. To our knowledge, this library stands as the most comprehensive and systematic array of sulfated fucoidans reported to date. Our detailed analysis of the structural and anticoagulant properties of these molecules has revealed key insights into previously poorly understood structure-activity relationships. Each parameter investigated, including molecular size, glycosidic bond connectivity, and specific sulfation pattern, was shown to play a crucial role in anticoagulant efficacy. For Type A compounds, the modification of 2,3,4-*O*-tri-sulfation significantly enhanced anticoagulant activity. Similarly, in Type B compounds, both 2,3-*O*-di-sulfation and 2,3,4-*O*-tri-sulfation modifications yielded superior anticoagulant effects, with efficacy improving as molecular size increases. Fucoidans **29**, **30**, **37**, and **58** exhibited exceptional anticoagulant properties, rivaling commercially available options such as enoxaparin. Notably, these compounds demonstrate a unique mechanism of anticoagulation by selectively modulating the intrinsic coagulation pathway. This targeted approach will provide enhanced precision in anticoagulant therapy, promising a safer and more controllable therapeutic profile. Such specificity not only mitigates the risks of bleeding but also offers potential advantages for tailored treatment in particular patient populations and clinical situations. While conventional anticoagulants provide broad-spectrum inhibition, the molecules developed in this study offer promising alternatives that could pave the way for more personalized and adaptable treatment strategies. This research underscores the potential for marine-derived molecules to inspire novel pharmaceuticals, thereby expanding the horizons of drug discovery and therapeutic innovation.

Methods

General

The experimental details and compound characterization data can be found in Supplementary Information. For the NMR and MS data of the compounds in the article, see Supplementary Information.

General procedure for the preactivation-based one-pot glycosylation reaction

A mixture of glycosyl donor, TTBP, and freshly activated 4 Å molecular sieves in anhydrous CH_2Cl_2 under argon atmosphere was stirred for 20 min at room temperature and then cooled to -78°C (or -72°C). After 5 min, AgOTf (dissolved in anhydrous toluene) was added to the mixture, followed by the addition of the stoichiometric amount of *p*-TolSCI. After TLC indicated the disappearance of the donor, a solution of glycosyl acceptor in anhydrous CH_2Cl_2 was slowly added. The resulting mixture was slowly warmed to room temperature within 2 h, stirred for another 20 min, and then cooled back to -78°C (or -72°C). The glycosylation operation mentioned above was repeated until the generation of the desired product.

Reporting summary

Further information on research design is available in the Nature Portfolio Reporting Summary linked to this article.

Data availability

All data supporting the results and conclusions are available within the article, its Supplementary Information, and from the corresponding authors upon request. Source data are provided in this paper.

References

- Mackman, N., Bergmeier, W., Stouffer, G. A. & Weitz, J. I. Therapeutic strategies for thrombosis: new targets and approaches. *Nat. Rev. Drug Discov.* **19**, 333–352 (2020).
- Xia, X., Cai, X., Chen, J., Jiang, S. & Zhang, J. Construction of warfarin population pharmacokinetics and pharmacodynamics model in Han population based on Bayesian method. *Sci. Rep.* **14**, 14846–14855 (2024).

3. Deng, J. Q. et al. Biosynthetic production of anticoagulant heparin polysaccharides through metabolic and sulfotransferases engineering strategies. *Nat. Commun.* **15**, 3755 (2024).
4. Kumano, O., Akatsuchi, K. & Amiral, J. Updates on anticoagulation and laboratory tools for therapy monitoring of heparin, vitamin K antagonists and direct oral anticoagulants. *Biomedicines* **9**, 264–284 (2021).
5. Ushakova, N. A. et al. Anticoagulant activity of fucoidans from brown algae. *Biochem. Suppl. Ser. B Biomed. Chem.* **3**, 77–83 (2009).
6. Van Weelden, G. et al. Fucoidan structure and activity in relation to anti-cancer mechanisms. *Mar. Drugs* **17**, 32–62 (2019).
7. Apostolova, E. et al. Immunomodulatory and anti-inflammatory effects of fucoidan: a review. *Polymers* **12**, 12–24 (2020).
8. Queiroz, K. C. S. et al. Inhibition of reverse transcriptase activity of HIV by polysaccharides of brown algae. *Biomed. Pharmacother.* **62**, 303–307 (2008).
9. Shang, F. et al. Structural analysis and anticoagulant activities of three highly regular fucan sulfates as novel intrinsic factor Xase inhibitors. *Carbohydr. Polym.* **195**, 257–266 (2018).
10. Sun, X. et al. Orally administrated fucoidan and its low-molecular-weight derivatives are absorbed differentially to alleviate coagulation and thrombosis. *Int. J. Biol. Macromol.* **255**, 128092 (2024).
11. Qi, Y. et al. Preparation of low-molecular-weight fucoidan with anticoagulant activity by photocatalytic degradation method. *Foods* **11**, 822–834 (2022).
12. Collic, S. et al. Anticoagulant properties of a fucoidan fraction. *Thromb. Res.* **64**, 143–154 (1991).
13. Vilela-Silva, A.-C. E. S., Castro, M. O., Valente, A.-P., Biermann, C. H. & Mourão, P. A. S. Sulfated fucans from the egg jellies of the closely related sea urchins *Strongylocentrotus droebachiensis* and *Strongylocentrotus pallidus* ensure species-specific fertilization. *J. Biol. Chem.* **277**, 379–387 (2002).
14. Luthuli, S. et al. Therapeutic effects of fucoidan: a review on recent studies. *Mar. Drugs* **17**, 487–502 (2019).
15. Koike, T. et al. Synthesis of low-molecular weight fucoidan derivatives and their binding abilities to SARS-CoV-2 spike proteins. *RSC Med. Chem.* **12**, 2016–2021 (2021).
16. Sugimoto, A. et al. Synthesis of low-molecular-weight fucoidan analogue and its inhibitory activities against heparanase and SARS-CoV-2 infection. *Angew. Chem. Int. Ed.* **64**, e202411760 (2024).
17. Kasai, A., Arafuka, S., Koshiba, N., Takahashi, D. & Toshima, K. Systematic synthesis of low-molecular weight fucoidan derivatives and their effect on cancer cells. *Org. Biomol. Chem.* **13**, 10556–10568 (2015).
18. Kosono, S. et al. Novel hemagglutinin-binding sulfated oligofucosides and their effect on influenza virus infection. *Chem. Commun.* **54**, 7467–7470 (2018).
19. Arafuka, S., Koshiba, N., Takahashi, D. & Toshima, K. Systematic synthesis of sulfated oligofucosides and their effect on breast cancer MCF-7 cells. *Chem. Commun.* **50**, 9831–9834 (2014).
20. Xu, Z. et al. Integrated chemoenzymatic synthesis of a comprehensive sulfated ganglioside glycan library to decipher functional sulfoglycomics and sialoglycomics. *Nat. Chem.* **16**, 881–892 (2024).
21. Ramadan, S. et al. Recent advances in the synthesis of extensive libraries of heparan sulfate oligosaccharides for structure–activity relationship studies. *Curr. Opin. Chem. Biol.* **80**, 102455 (2024).
22. Tan, Z. et al. A comprehensive synthetic library of poly-*N*-acetyl glucosamines enabled vaccine against lethal challenges of *Staphylococcus aureus*. *Nat. Commun.* **15**, 3420 (2024).
23. Wang, L. et al. Efficient platform for synthesizing comprehensive heparan sulfate oligosaccharide libraries for decoding glycosaminoglycan-protein interactions. *Nat. Chem.* **15**, 1108–1117 (2023).
24. Li, Z. et al. Synthetic O-acetylated sialosides facilitate functional receptor identification for human respiratory viruses. *Nat. Chem.* **13**, 496–503 (2021).
25. Krasnova, L. & Wong, C.-H. Oligosaccharide synthesis and translational innovation. *J. Am. Chem. Soc.* **141**, 3735–3754 (2019).
26. Crawford, C. J. et al. Automated synthesis of algal fucoidan oligosaccharides. *J. Am. Chem. Soc.* **146**, 18320–18330 (2024).
27. Vinnitskiy, D. Z., Krylov, V. B., Ustyuzhanina, N. E., Dmitrenok, A. S. & Nifantiev, N. E. The synthesis of heterosaccharides related to the fucoidan from *Chordaria flagelliformis* bearing an α -L-fucofuranosyl unit. *Org. Biomol. Chem.* **14**, 598–611 (2016).
28. Yao, W. & Ye, X.-S. Donor preactivation-based glycan assembly: from manual to automated synthesis. *Acc. Chem. Res.* **57**, 1577–1594 (2024).
29. Ma, Y. et al. One-pot assembly of mannose-capped lipoo-abinomannan motifs up to 101-mer from the *Mycobacterium tuberculosis* cell wall. *J. Am. Chem. Soc.* **146**, 4112–4122 (2024).
30. Qin, X. et al. Synthesis of branched arabinogalactans up to a 140-mer from *Panax notoginseng* and their anti-pancreatic-cancer activity. *Nat. Synth.* **3**, 245–255 (2024).
31. Yao, W. et al. Automated solution-phase multiplicative synthesis of complex glycans up to a 1,080-mer. *Nat. Synth.* **1**, 854–863 (2022).
32. Zhu, Q. et al. Chemical synthesis of glycans up to a 128-mer relevant to the O-antigen of *Bacteroides vulgatus*. *Nat. Commun.* **11**, 4142 (2020).
33. Joseph, A. A., Pardo-Vargas, A. & Seeberger, P. H. Total synthesis of polysaccharides by automated glycan assembly. *J. Am. Chem. Soc.* **142**, 8561–8564 (2020).
34. Wu, Y., Xiong, D.-C., Chen, S.-C., Wang, Y.-S. & Ye, X.-S. Total synthesis of mycobacterial arabinogalactan containing 92 monosaccharide units. *Nat. Commun.* **8**, 14851 (2017).
35. Zhang, Y. et al. Merging reagent modulation and remote anchimeric assistance for glycosylation: highly stereoselective synthesis of α -glycans up to a 30-mer. *Angew. Chem. Int. Ed.* **60**, 12597–12606 (2021).
36. Huang, X., Huang, L., Wang, H. & Ye, X.-S. Iterative one-pot synthesis of oligosaccharides. *Angew. Chem. Int. Ed.* **43**, 5221–5224 (2004).
37. Qin, X. & Ye, X.-S. Donor preactivation-based glycosylation: an efficient strategy for glycan synthesis. *Chin. J. Chem.* **39**, 531–542 (2021).
38. Liu, M., Qin, X. & Ye, X.-S. Glycan assembly strategy: from concept to application. *Chem. Rec.* **21**, 3256–3277 (2021).
39. Yang, B., Yang, W., Ramadan, S. & Huang, X. Pre-activation based stereoselective glycosylations. *Eur. J. Org. Chem.* **2018**, 1075–1096 (2018).
40. Grover, S. P. & Mackman, N. Intrinsic pathway of coagulation and thrombosis insights from animal models. *Arterioscler Thromb. Vasc. Biol.* **39**, 331–338 (2019).
41. Wang, J., Zhang, Q., Zhang, Z. & Li, Z. Antioxidant activity of sulfated polysaccharide fractions extracted from *Laminaria japonica*. *Int. J. Biol. Macromol.* **42**, 127–132 (2008).
42. Li, B.-H. et al. Total synthesis of tumor-associated KH-1 antigen core nonasaccharide via photo-induced glycosylation. *Org. Chem. Front.* **7**, 1255–1259 (2020).
43. Wang, Y.-S., Wu, Y., Xiong, D.-C. & Ye, X.-S. Total synthesis of a hyperbranched *N*-linked hexasaccharide attached to ATCV-1 major capsid protein without precedent. *Chin. J. Chem.* **37**, 42–48 (2019).
44. Wang, D., Xiong, D.-C. & Ye, X.-S. A five-component one-pot synthesis of phosphatidylinositol pentamannoside (PIM5). *Chin. Chem. Lett.* **29**, 1340–1342 (2018).
45. Hansen, T. et al. Characterization of glycosyl dioxolenium ions and their role in glycosylation reactions. *Nat. Commun.* **11**, 2664 (2020).
46. Zhang, Z. et al. Programmable one-pot oligosaccharide synthesis. *J. Am. Chem. Soc.* **121**, 734–753 (1999).

47. Komadsson, P., Udodong, U. E. & Fraser-Reid, B. Iodonium promoted reactions of disarmed thioglycosides. *Tetrahedron Lett.* **31**, 4313–4316 (1990).
48. Veeneman, G. H., van Leeuwen, S. H. & van Boom, J. H. Iodonium promoted reactions at the anomeric center. II. An efficient thioglycoside mediated approach toward the formation of 1,2-*trans* linked glycosides and glycosidic esters. *Tetrahedron Lett.* **31**, 1331–1334 (1990).
49. Codée, J. D. C. et al. Ph₂SO/Tf₂O: a powerful promotor system in chemoselective glycosylations using thioglycosides. *Org. Lett.* **5**, 1519–1522 (2003).
50. Crich, D. & Smith, M. 1-Benzenesulfinyl piperidine/tri-fluoromethanesulfonic anhydride: a potent combination of shelf-stable reagents for the low-temperature conversion of thioglycosides to glycosyl triflates and for the formation of diverse glycosidic linkages. *J. Am. Chem. Soc.* **123**, 9015–9020 (2001).
51. Wang, C., Wang, H., Huang, X., Zhang, L.-H. & Ye, X.-S. Benzene-sulfinyl morpholine: a new promoter for one-pot oligosaccharide synthesis using thioglycosides by pre-activation strategy. *Synlett* **2006**, 2846–2850 (2006).
52. Ahmad, S.-S., Rawala-Sheikh, R. & Walsh, P.-N. Components and assembly of the factor X activating complex. *Semin. Thromb. Hemost.* **18**, 311–323 (1992).

Acknowledgements

This work was financially supported by the grants from the National Natural Science Foundation of China (22237001 (X.-S.Y.), 22227801 (X.-S.Y.), 81930097 (M.W.), 82473811 (M.W.)), the National Key Research and Development Program of China (2022YFC3400800 (X.-S.Y.)), Yunnan Fundamental Research Projects (202201AS070073 (M.W.), 202301AV070008 (M.W.), 202302AA310012 (M.W.)), and Postdoctoral Directional Training Foundation of Yunnan Province (L.L.). We thank Dr. Yuan Wang and Dr. Fen Liu at Peking University Health Science Center for their assistance in analysis of glycan structures. We thank Chandler Wells and Rohan P. Patel at the University of Texas at Austin for language editing.

Author contributions

X.-S.Y. conceived the research. X.-S.Y., S.-C.C., and M.W. designed the experiments. S.-C.C. performed most of the synthetic experiments. N.X. and L.L. performed biological evaluation experiments. Y.W., Q.L., and D.S. performed partial chemistry experiments. X.Q., S.-C.C., X.-S.Y., and M.W. analyzed the data. X.Q. and X.-S.Y. wrote the manuscript. D.-C.X.

and C.E.C. discussed the data analysis and revised the manuscript. M.W. guided the biological assay. X.-S.Y. supervised the project.

Competing interests

X.-S.Y., S.-C.C., and M.W. are applying for a Chinese patent filed by Peking University and Kunming Institute of Botany, Chinese Academy of Sciences. The other authors declare no competing interests.

Additional information

Supplementary information The online version contains supplementary material available at <https://doi.org/10.1038/s41467-025-59632-2>.

Correspondence and requests for materials should be addressed to Mingyi Wu or Xin-Shan Ye.

Peer review information *Nature Communications* thanks Tiehai Li, Jian Liu, and the other anonymous reviewer(s) for their contribution to the peer review of this work. A peer review file is available.

Reprints and permissions information is available at <http://www.nature.com/reprints>

Publisher's note Springer Nature remains neutral with regard to jurisdictional claims in published maps and institutional affiliations.

Open Access This article is licensed under a Creative Commons Attribution-NonCommercial-NoDerivatives 4.0 International License, which permits any non-commercial use, sharing, distribution and reproduction in any medium or format, as long as you give appropriate credit to the original author(s) and the source, provide a link to the Creative Commons licence, and indicate if you modified the licensed material. You do not have permission under this licence to share adapted material derived from this article or parts of it. The images or other third party material in this article are included in the article's Creative Commons licence, unless indicated otherwise in a credit line to the material. If material is not included in the article's Creative Commons licence and your intended use is not permitted by statutory regulation or exceeds the permitted use, you will need to obtain permission directly from the copyright holder. To view a copy of this licence, visit <http://creativecommons.org/licenses/by-nc-nd/4.0/>.

© The Author(s) 2025